RSC Advances

This article can be cited before page numbers have been issued, to do this please use: L. javadian and J. Safari, *RSC Adv.*, 2015, DOI: 10.1039/C5RA23457C.

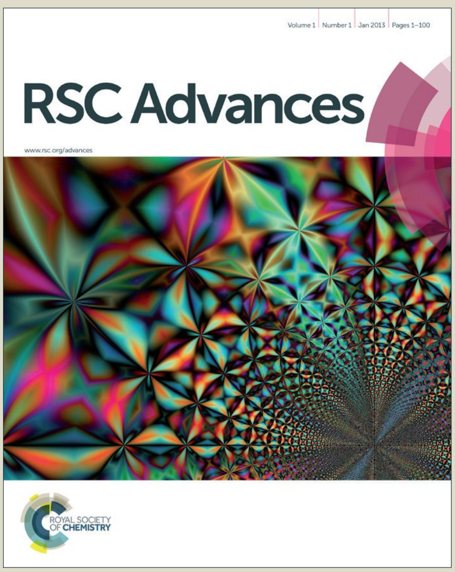

View Article Online
DOI: 10.1039/C5RA23457C

Journal Name

ARTICLE

An efficient synthesis of perhydro[1,2,4]triazolo[1,2-a][1,2,4] triazole-1,5-dithiones catalyzed by TiO_2-functionalized nano-Fe_3O_4 encapsulated-silica particles as a reusable magnetic nanocatalyst

Received 00th January 20xx,
Accepted 00th January 20xx

DOI: 10.1039/x0xx00000x

www.rsc.org/

Javad Safari, and Leila Javadian

Immobilization of a nano-TiO_2 catalyst on the surface of a magnetic SiO_2support was performed through the reaction of Fe_3O_4@SiO_2 composite with $Ti(OC_4H_9)_4$ *via* a simple process. The Fe_3O_4@SiO_2–TiO_2 nanocomposite was characterized using scanning electron microscopy (SEM), transmission electron microscopy (TEM), energy dispersive X-ray spectroscopy (EDS), X-ray diffraction (XRD), Fourier transform infrared spectra (FTIR), and vibrating sample magnetometer (VSM). The Fe_3O_4@SiO_2–TiO_2 nanocomposite has been found to be an efficient catalyst for the synthesis of perhydro[1,2,4]triazolo[1,2-a][1,2,4] triazole-1,5-dithiones from the condensation of various aldazines and potassium thiocyanate in acetonitrile solvent at room temperature. It has been found that the nanocatalyst was recycled for up to 6 cycles with minimal loss in catalytic activity. The purpose of this research was to provide an easy method for the synthesis of perhydrotriazolotriazole derivatives by a robust and magnetic recoverable catalyst.

1. Introduction

1,3-Dipolar cycloaddition or [3+2] cycloaddition reaction is fundamental processes in organic chemistry that offers a powerful synthetic methodology to achieve five-membered heterocyclic systems in stereo and regiocontrolled approach.[1-4] The term "criss-cross" cycloaddition appeared in 1917 by Bailey and McPherson and the first paper described the cycloaddition of cyanic acid to benzalazine.[5] Criss-cross cycloaddition reactions are a procedure for the synthesis of fused heterocyclic rings in an one pot arrangement that offer two fused five-membered rings.[6,7] The formation of corresponding products was described by Huisgen as the result of two following 1,3-dipolar cycloadditions in 1963.[8] Since then, some papers have published listing examples of criss-cross cycloaddition reactions of aldazines and different dipolarophiles such as thiocyanate.[9] In addition to aldazines, the current reactions have been reported for ketazines[10] 1,2-diazabuta-1,3-dienes,[11, 12] glyoxalimines,[13] and hexafluoroacetonazine with many types of compounds including alkenes.[14] The 1,3-dipolar ketazines and aldazines are 1,3-heterodiene compounds and have double 1,3-dipolar sites (scheme 1).

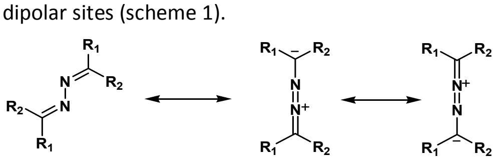

R_1= H, CH_3, ...

R_2= Alkyl, Aryl

Scheme 1. Azines containing double 1,3-dipolar sites.

Laboratory of Organic Compound Research, Department of Organic Chemistry, Faculty of Chemistry,University of Kashan, Kashan, P.O.Box: 87317-51167, Kashan, Iran. Tel:+9831-55912320; E-mail: Safari@kashanu.ac.ir

† Electronic Supplementary Information (ESI) available: See DOI: 10.1039/x0xx00000x

They adopt the s-trans conformation due to steric interaction of the alkyl or aryl substations. So, this conformation does not suffer the [4+2] cycloaddition known as the Diels-Alder reaction.[15] Although, there are a few papers in the literatures that have described the synthesis of perhydrotriazolotriazoledithione derivatives, they have drawbacks such as high catalyst loading, drastic conditions, low yields and long reaction times.[16,17]

In recent decades, design of magnetically catalysts has attracted a great deal of attention due to simple separation of catalysts by a permanent magnetic field. A lot of materials such as FeCo, Fe_2O_3, $NiFe_2O_4$, Fe_3O_4, $CoFe_2O_4$ and black sand have the magnetic properties.[18-23] Among them, Fe_3O_4 nanoparticles has been chosen because of its low toxicity and remarkable magneticproperties.[24-26] Fe_3O_4 nanoparticles have emerged as supports for immobilization of catalyst which offer an easy separation of the catalyst without the need of conventional filtration method or tedious work-up processes. Beside the facile separation, a great feature of Fe_3O_4 nanoparticles is their surface modification that affords sometimes higher activity than their homogeneous systems. Fe_3O_4 core with shell of silica offers sites for surface modification with various compounds in catalyst application. Silica layer not only avoids the oxidation of the Fe_3O_4 by the outer atmosphere, but also can prevent the aggregation induced by the magnetic dipolar attraction between magnetic nanoparticles.[27-29] Also, silica enhances a better dispersion of magnetic nanoparticles in suspension.[30] Magnetic nanoparticles have been used as catalysts or catalyst supports in many organic reactions including oxidation, reductions, multicomponent reactions and C-C couplings with a high level of activity.[31-34] It is anticipated that the magnetic properties of catalyst would be useful to improve the performance of the [3+2] cycloaddition reaction and provide a support for the solid acid catalyst. On the other side, extensive attention has been directed toward the application of solid acids in organic synthesis because such reagents help prevent release of reaction residues into the environment. In this regard, nanostructure solid acids show higher

View Article Online
DOI: 10.1039/C5RA23457C

activity than their bulk materials due to their particular chemical and physical properties especially large surface to volume ratio.[35] As an extension of our researches on the application of magnetic solid acids in organic transformations, functionalization of Fe_3O_4 nanoparticles with TiO_2 has been studied to offer magnetic catalyst which combines the benefits of TiO_2 and Fe_3O_4 to afford greater potential applications.
In this contribution, we hope to report an efficient method for the synthesis of perhydrotriazolotriazoledithions by the condensation of aldazines as 1,3-heterodienes with thiocyanate in [3+2] cycloaddition by a magnetically recyclable catalyst.

2. Experimental

2.1. General

All the commercially available reagents were obtained from Aldrich or Merk and were used without further purification. ^{1}H and ^{13}C NMR spectra were recorded on a Bruker DRX-400 spectrometer. Chemical shifts are expressed in δ parts per million. The IR spectra of the compounds were recorded on a Perkin Elmer FT-IR 550 spectrophotometer. All melting points (m.p.) were determined on an ElectroMK3 apparatus, expressed in °C and are uncorrected. Analytical thin layer chromatography (TLC) on silica gel plates containing UV indicator was employed regularly to follow the course of reactions and to confirm the purity of products. The Sonication was performed in Shanghai Branson-BUG40-06 ultrasonic cleaner. The obtained nanoparticles were characterized by XRD on a Bruker D8 Advance X-ray diffraction (XRD) diffractometer (CuK, radiation, k =0.154056 nm and 40 kV voltage), at a scanning speed of 2° min^{-1} from 10° to 100° (2ɵ). Scanning electron microscope (SEM) was performed on a FEI Quanta 200 SEM operated at a 20 kV accelerating voltage. Magnetic properties were characterized by a vibrating sample magnetometer (VSM, MDKFD, University of kashan, Kashan, Iran) at room temperature. The samples for SEM were prepared by spreading a small drop containing nanoparticles onto a silicon wafer and being dried almost completely in air at room temperature for 2 h, and then were transferred onto SEM conductive tapes. The TEM images were recorded usinga Ziess EM10C transmission electron microscope operated at a 80 KV accelerating votage.

2.2. Preparation of Fe_3O_4@SiO_2 as a support

First, Fe_3O_4 nanoparticles were prepared by chemical co-precipitation of $FeCl_2$ and $FeCl_3$[Fe^{2+}: Fe^{3+}= 1:2] in base solution as described in the literature.[36, 37] Then, Fe_3O_4-SiO_2 composite were synthesized through the Stöber method using tetraethyl orthosilicate as a silica source in a basic water/ethanol mixture at room temperature under continuous mechanical stirring.[38] Briefly, 0.5 g of the Fe_3O_4nanoparticles was dispersed in 20 ml of distilled water and 50 ml of ethanol under ultrasound irradiation and then concentrated aqueous ammonia (1 ml) was added. Finally, 0.2 ml of tetraethyl orthosilicate diluted in ethanol (10 ml) was added drop-wisely under continuous mechanical stirring. After stirring for 18 h, Fe_3O_4@SiO_2 nanoparticles were collected by magnetic separation and washed three times with water and ethanol. Finally, the magnetic product was dried at 70 °C for 6 h.

2.3. Preparation of catalyst

A magnetically separable TiO_2 catalyst was prepared by dissolving 1.5 ml of $Ti(OC_4H_9)_4$ in 30 ml ethanol and adding this solution dropwise into a mixture containing 0.40 g of magnetic Fe_3O_4@SiO_2 in 10 ml water/ethanol. The mixture was refluxed at 90 C for about 2 h. Then, the magnetic sample was dried at 60 °C and calcined at 450 °C for 2 h to offer Fe_3O_4@SiO_2-TiO_2 nanocomposite.[39]

2.4. A typical procedure for the synthesis of aldazines

Aldazines were prepared by the method as described in the literature.[40] A mixture of the aldehyde (2 mmol), hydrazine sulfate (1 mmol), and triethylamine (1 mmol) was heated at 60 °C for 3–5 min. The completion of the reaction was monitored by thin layer chromatography (petroleum ether:ethyl acetate= 7:3).After the completion of the reaction, the mixture was cooled on ice. The aldazine was collected by suction filtration. Then, it was washed with water, and dried under vacuum. The yellow solid was recrystallized from ethanol to afford the desired aldazineas cream to orange crystals.

2.5. A typical procedure for the synthesis of tetrahydro-[1,2,4] triazolo [1,2-a][1,2,4]triazole-1,5-dithione derivatives

In a typical experiment, KSCN (2 mmol), AcOH (0.18 mL), CH_3CN (6 mL) and catalytic amount of Fe_3O_4@SiO_2-TiO_2nanocomposite (0.04 g) were stirred at room temperature. After stirring for 5 min, aldazine (1 mmol) was added to this mixture and the contents were stirred for an appropriate period while the progress of the reaction was followed by TLC using petroleum ether:ethyl acetate=7:3) as eluent. After completion of the reaction, the nanocatalyst was removed by an external magnet and reused. Then, cold water (50 mL) was added and the solid product was collected by filtration, was washed successively with $CHCl_3$, dried and recrystallized from ethanol to afford the pure product. The products were identified by comparison of their spectroscopic and physical data with those reported in the literature.

2.5.1. Spectral data for compounds

2.5.1.1. Tetrahydro-3,7-diphenyl-[1,2,4] triazolo [1,2-a] [1,2,4] triazole-1,5-dithione (**3a**): white solid, m.p= 188-189 °C; R_f (petroleum ether:ethylacetate= 7:3 (v/v)) = 0.26; IR (KBr)/ ν (cm^{-1}): 3385, 3180, 1500, 1251; ^{1}H NMR (Acetone-d_6, 400 MHz)/ δ ppm:6.81 (s, 2H, CH), 7.38-7.42 (m, 10H, Ar-H), 11.42 (s, 2H, NH);^{13}C NMR (DMSO-d_6, 100 MHz) δ (ppm): 73 (CH), 126.25 (CH), 127.76 (CH), 128.31 (CH), 129.73 (CH), 184.1 (C=S) ppm; $CHN_{Calculated}$ (%): C (58.89), H (4.29), N (17.18), S (19.63); CHN_{Found} (%): C (58.82), H (4.39), N (17.34), S (19.73).[17]

2.5.1.2. Tetrahydro-3,7-bis (3-nitrophenyl)-[1,2,4] triazolo [1,2-a] [1,2,4] triazole-1,5-dithione (**3b**): white solid, m.p= 190-191 °C; R_f (petroleum ether:ethylacetate= 7:3 (v/v)) =0.15; IR (KBr)/ ν (cm^{-1}): 3215, 1616, 1529, 1491, 1352, 1247, 1161; ^{1}H NMR (Acetone-d_6, 400 MHz)/ δ ppm:7.25 (s, 2H, CH), 7.80 (t, *J*= 7.0 Hz, 2H, ArH), 8.00 (d, *J*= 7.0 Hz, 2H, ArH), 8.31 (d, *J*= 7.0 Hz, 2H, ArH), 8.39 (s, 2H, ArH), 10.38 (s, 2H, NH) ppm;);^{13}C NMR (Acetone-d_6, 100 MHz) δ (ppm): 72.0 (CH), 119.43 (CH), 122.55 (CH), 129.88 (CH), 133.76 (CH), 145.50 (CH), 148.60 (C), 158.09 (C), 184.11 (C=S) ppm; $CHN_{Calculated}$ (%):C (46.02), H (2.2.87), N (20.13), S (15.62), O (15.36); CHN_{Found} (%): C (46.45), H (3.01), N (19.18), S (15.35), O (16.01).

2.5.1.3. Tetrahydro-3,7-bis (4-methoxyphenyl)-[1,2,4] triazolo [1,2-a] [1,2,4] triazole-1,5-dithione (**3c**): white solid, m.p= 160-162 °C; R_f (petroleum ether:ethylacetate= 7:3 (v/v)) =0.18; IR (KBr)/ υ(cm^{-1}): 3390, 3157, 2960, 1613, 1508, 1249, 1173, 1028; ^{1}H NMR (Acetone-

View Article Online
DOI: 10.1039/C5RA23457C

d$_6$, 400 MHz)/ δ ppm: 3.72 (s, 6H, OCH_3), 6.75 (s, 2H, CH), 6.99 (s, 4H, Ar-H), 7.28-7.30 (d,J= 6.8 Hz, 4H, Ar-H), 11.31 (s, 2H, NH) ppm; ^{13}C NMR (DMSO-*d*$_6$, 100 MHz) δ (ppm): 55.73 (CH3), 77.03 (CH), 114.76 (CH), 127.67 (CH), 130.0 (C), 160.35 (C), 184.0 (C=S); ppm; $CHN_{Calculated}$ (%): C (55.96), H (4.66), N (14.51), S (16.58); CHN_{Found} (%): C (55.93), H (4.76), N (14.72), S (16.68).[17]

2.5.1.4. Tetrahydro-3,7-bis (2-chlorophenyl)-[1,2,4] triazolo [1,2-a] [1,2,4] triazole-1,5-dithione **(3d):**white solid, m.p= 197 °C; R_f (petroleum ether:ethylacetate= 7:3 (v/v)) =0.32; IR (KBr) ν (cm^{-1}): 3433, 3183, 2929, 1498,1251; ^1H NMR (DMSO-*d*$_6$, 400 MHz) δ (ppm): 7.16 (s, 1H, CH), 7.34-7.36 (m, 1H, Ar-H), 7.43-7.47 (m, 2H, Ar-H), 7.54-7.61 (m, 1H, Ar-H), 11.48 (s, 1H, NH); ^{13}C NMR (DMSO-*d*$_6$, 100 MHz) δ (ppm): 74.86 (CH), 128.14 (CH), 128.63 (CH), 130.62 (CH), 131.87 (CH), 132.48 (C), 134.01 (C), 185.19 (C=S) ppm; $CHN_{Calculated}$ (%): C (48.60), H (3.04), N (14.18), S (16.20), Cl (17.72); CHN_{Found} (%): C (47.99), H (3.58), N (14.76), S (16.09), Cl (17.58).

*2.5.1.5.*Tetrahydro-3,7-bis (3-chlorophenyl)-[1,2,4] triazolo [1,2-a] [1,2,4] triazole-1,5-dithione (**3e**): white solid, m.p= 194-195 °C; R_f (petroleum ether:ethylacetate= 7:3 (v/v)) = 0.35; IR (KBr)/ ν (cm^{-1}): 3427, 3191, 2927, 1501, 1247 ;^1H NMR (Acetone-*d*$_6$, 400 MHz)/ δ ppm: 7.07 (s, 1H, CH), 7.47-7.51 (m, 3H, Ar-H), 7.55 (s, 1H, Ar-H), 10.14 (s, 1H, NH);^{13}C NMR (DMSO-*d*$_6$, 100 MHz) δ (ppm): 76.62 (CH), 124.88 (CH), 126.39 (CH), 128.12 (CH), 131.84 (CH), 134.15 (C), 139.76 (C), 184.47 (C=S) ppm; $CHN_{Calculated}$ (%): C (48.60), H (3.04), N (14.18), S (16.20), Cl (17.72); CHN_{Found} (%): C (48.32), H (3.13), N (14.31), S (16.29), Cl (17.81).[17]

2.5.1.6. Tetrahydro-3,7-bis (4-chlorophenyl)-[1,2,4] triazolo [1,2-a] [1,2,4] triazole-1,5-dithione (**3f**): white solid, m.p= 201-203 °C; R_f (petroleum ether:ethylacetate)= 7:3 (v/v)) =0.31; IR (KBr)/ ν (cm^{-1}): 3438, 3168, 2925, 1629, 1492, 1249, 1157; ^1H NMR (Acetone-*d*$_6$, 400 MHz)/ δ ppm:6.84 (s, 2H, CH), 7.39 (s, 4H, ArH), 7.51 (s, 4H, ArH), 11.48 (s, 2H, NH) ppm;^{13}C NMR (DMSO-*d*$_6$, 100 MHz) δ (ppm): 75.50 (CH), 128.4 (CH), 130.45 (CH), 133.21 (CH), 133.8 (CH), 184.1 (C=S) ppm; $CHN_{Calculated}$ (%): C (48.60), H (3.04), N (14.18), S (16.20), Cl (17.72); CHN_{Found} (%): C (58.82), H (4.39), N (17.34), S (19.73).[17]

2.5.1.7. Tetrahydro-3,7-bis (3-hydroxyphenyl)-[1,2,4] triazolo [1,2-a] [1,2,4] triazole-1,5-dithione (**3g**): white solid, m.p= 165-167 °C; R_f (petroleum ether:ethylacetate= 7:3 (v/v)) =0.12; IR (KBr)/ ν (cm^{-1}): 3423, 3177, 2958, 1601, 1505, 1250; ^1H NMR (Acetone-*d*$_6$, 400 MHz) δ (ppm): 6.95 (s, 4H, Ar-H), 7.24 (s, 1H, CH), 8.62 (s, 1H, OH), 9.97 (s, 1H, NH) ppm;^{13}C NMR (Acetone-*d*$_6$, 100 MHz) δ (ppm): 73 (CH), 112.01 (CH), 113. 88 (CH), 119.03 (CH), 130.0 (CH), 145.50 (CH), 158.09 (C), 184. 0 (C=S) ppm;$CHN_{Calculated}$ (%): C (53.70), H (3.88), N (15.04), S (17.68), O (9.70); CHN_{Found} (%): C (53.76), H (3.58), N (15.34), S (17.74), O (9.66).

2.5.1.8. Tetrahydro-3,7-bis (3-hydroxy-4-methoxyphenyl)-[1,2,4] triazolo [1,2-a][1,2,4]triazole-1,5-dithione (**3h**): white solid, m.p= 177-180 °C; R_f (petroleum ether:ethylacetate= 7:3 (v/v)) =0.06; IR (KBr)/ ν (cm^{-1}): 3422, 2929, 1510, 1278, 1133; ^1H NMR (Acetone-*d*$_6$, 400 MHz)/ δ ppm:3.81 (s, 6H, OCH_3), 6.86 (s, 2H, CH), 6.96-7.40 (m, 6H, ArH), 7.89 (s, 2H, OH), 9.88 (s, 2H, NH) ppm; ^{13}C NMR (Acetone-*d*$_6$, 100 MHz) δ (ppm): 55.40 (OCH_3), 77.09 (CH), 111.54 (CH), 112.79 (CH), 117.32 (CH), 129.98 (C), 146.91 (C), 148.37 (C), 185.00 (C=S);$CHN_{Calculated}$ (%): C (51.52), H (4.29), N (13.35), S (15.55), O (15.29); CHN_{Found} (%): C (51.34), H (4.83), N (12.88), S (14.98), O (15.97).

3. Results and discussion

3.1. Characterization of magnetic nanocatalyst

The synthetic path to the magnetic nanocatalyst is shown in Scheme 2.

Iron-oxide nanoparticles were prepared via co-precipitation and modified with a thin layer of amorphous silica by Stöber method through sol–gel method. The $Fe_3O_4@SiO_2$ -supported TiO_2 magnetic catalyst obtained after addition of $Ti(OC_4H_9)_4$ into the $Fe_3O_4@SiO_2$ magnetic composite. Silica layer was utilized to encapsulate the Fe_3O_4 NPs to prevent any decrease in catalytic property when it was incorporated into the TiO_2 structure. Because silica as a shell can decrease the electronic interactions at the point of contact.[19]

The magnetic nanoparticles were characterized by X-ray diffraction (XRD), Fourier transform infrared (FT-IR), scanning electron microscopy (SEM), energy-dispersive X-ray spectrometry (EDX), and vibrating sample magnetometer (VSM).

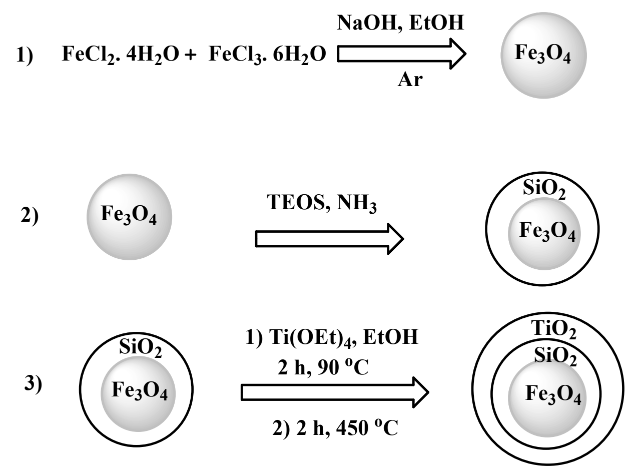

Scheme 2. Preparation steps of magnetic catalyst.

The phase and purity of three samples (Fe_3O_4, $Fe_3O_4@SiO_2$ and $Fe_3O_4@SiO_2$-TiO_2) were plotted by The X-ray diffraction patterns (Figure 1).

The XRD pattern of Fe_3O_4 MNPs exhibit the peaks at 2θ= 30.1, 35.5, 43.2, 53.5, 57.0, 62.8 and 74.3° (Figure 1a). It is in agreement with the JCPDS card No. 19–0629.[36]The coating of amorphous phase SiO_2 does not change the structure of Fe_3O_4nanoparticles (Figure 1b). Also, the position and relative intensities of peaks indicate that the structure of $Fe_3O_4@SiO_2$ can be remained after the surface modification with TiO_2. The XRD pattern of the $Fe_3O_4@SiO_2$-TiO_2 MNPs shows peaks at 2θ =25.2, 30.3, 35.6, 43.4, 48.2, 53.5, 57.2 63.1 and 74.4°(Figure1c). The peaks at around 25° and 48° conform to the (1 0 1) and (2 0 0) Bragg reflection planes which indicates the existence of tetragonal anatase TiO_2.

The elemental composition is calculated from the energy dispersive X-ray. The EDAX image confirmed the existence of Fe, Si, O and Ti elements in the magnetic catalyst (Figure 2). The elemental compositions of $Fe_3O_4@SiO_2$-TiO_2nanocatalystwere 14.9, 70.3, 6.7, and 7.9 wt % for Fe, O, Si, and Ti, respectively. The presence of Ti inthe composites indicates that the titanium dioxide nanoparticles have been deposited on the surface of $Fe_3O_4@SiO_2$.

View Article Online
DOI: 10.1039/C5RA23457C

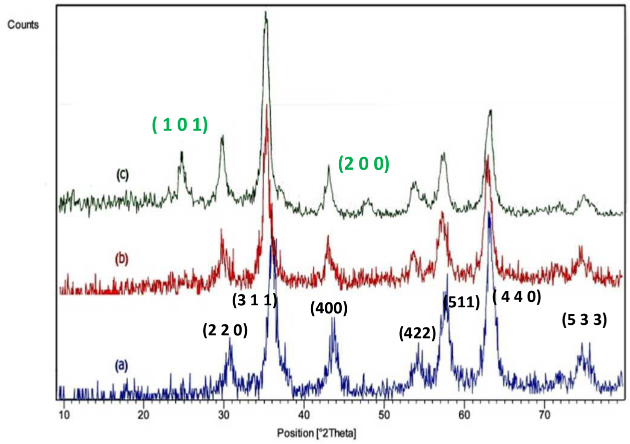

Figure 1. The XRD patterns of (a) Fe_3O_4 (b) Fe_3O_4@SiO_2 and (c) Fe_3O_4@SiO_2-TiO_2.

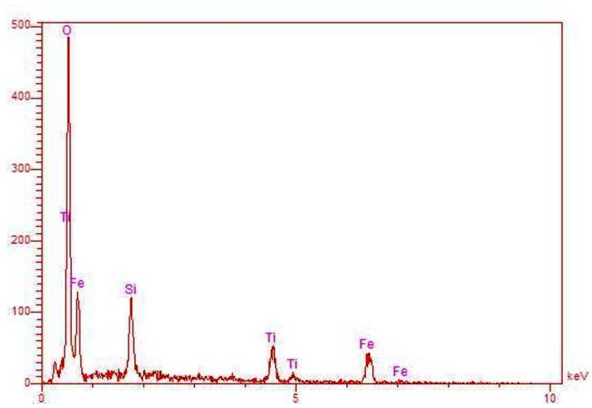

Figure 2. The EDAX of Fe_3O_4@SiO_2-TiO_2 nanocatalyst.

Scanning electron microscopy (SEM) and transmission electron microscopy (TEM) were recorded to understand morphological changes occurring on the magnetic catalyst and also the size and shape of the nanoparticles.

The SEM and TEM images of synthesized samples are shown in Figure 3. The SEM image of Fe_3O_4 MNPs have a mean diameter lower than 20 nm a nearly spherical shape (Figure 3a). Figure 3b shows that Fe_3O_4@SiO_2 nanoparticles keep the morphological properties of Fe_3O_4 MNPs except for a larger particle size and smoother surface. The TEM image shown in Fig. 3d demonstrates that silica is successfully coated on the Fe_3O_4NPs with a thin layer of different phase to form silica shell. So, Fe_3O_4@SiO_2 is nearly in core-shell structure.

Then, the chemical nature of the magnetic catalyst was surveyed. The SEM and TEM images in Fig. 3c and 3eshow that Fe_3O_4@SiO_2-TiO_2 nanocatalyst have a larger particle size than Fe_3O_4@SiO_2nanoparticles (about 30 nm in size) and nearly spherical shape. The nanocatalyst shows some aggregation, which was due to calcination at 450 °C.[39]

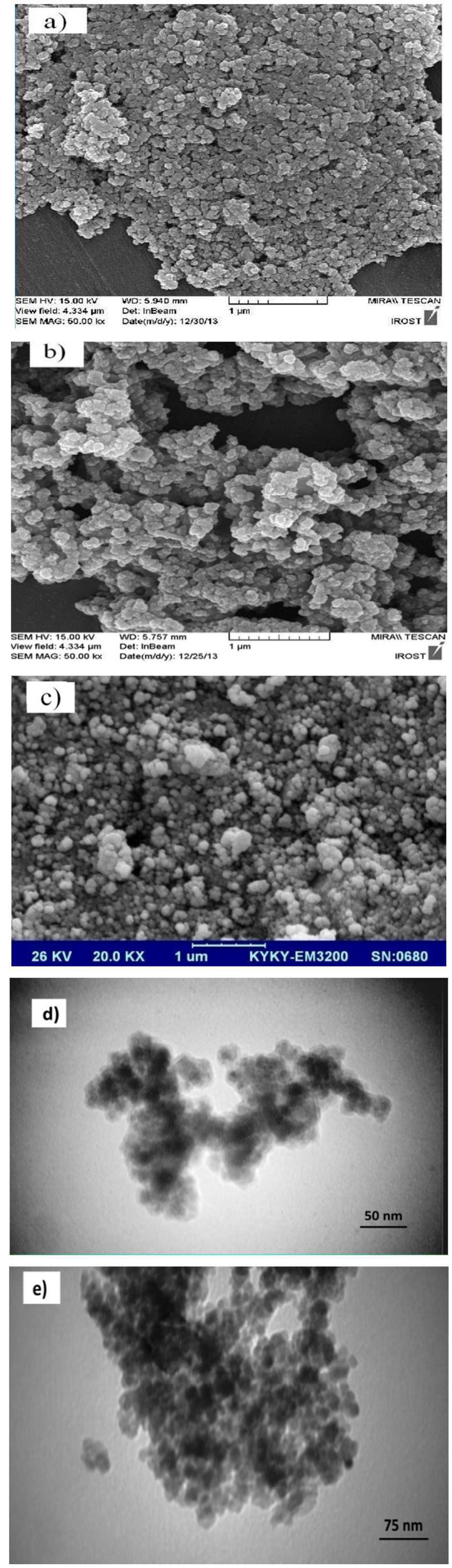

Figure 3. SEM image of the a) Fe_3O_4, b) Fe_3O_4@$SiO_2$and c) Fe_3O_4@SiO_2-TiO_2. TEM image of the d) Fe_3O_4@SiO_2 and e) Fe_3O_4@SiO_2-TiO_2.

View Article Online
DOI: 10.1039/C5RA23457C

In order to explore the molecular structures of Fe_3O_4, Fe_3O_4@SiO_2, and Fe_3O_4@SiO_2– TiO_2, the FT-IR analysis was investigated. Figure 4 shows the FT-IR spectra recorded in the range of 4000–400 cm^{-1}. The main absorption peaks 3423 and 570 cm^{-1} were assigned to O-H and Fe-O stretching vibration modes of pure Fe_3O_4 NPs, respectively (Figure 4a). The absorption peak of SiO_2-coated sample at 450 cm^{-1} is due to the Si-O-Fe bond.

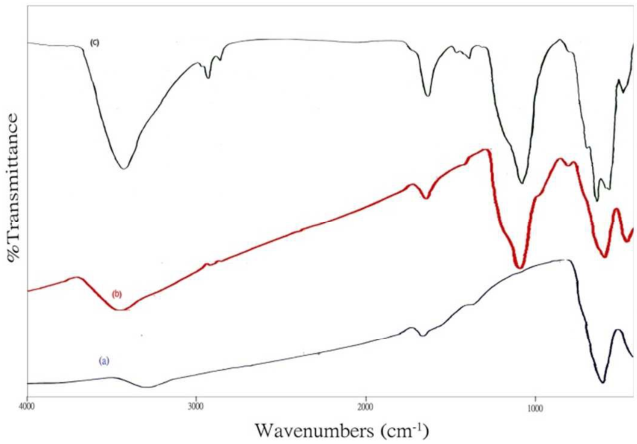

Figure 4. FT-IR spectra of (a) Fe_3O_4, (b) Fe_3O_4@SiO_2 and (c) Fe_3O_4@SiO_2-TiO_2.

The bands at 1073 cm^{-1} and 803 cm^{-1} are characteristic peaks of the symmetrical and asymmetrical vibrations of Si-O-Si (Figure 4b). The peak at 451 cm^{-1} is an indication of the presence of Si-O-Fe. Figure 4c show the IR spectra of TiO_2 modified Fe_3O_4@SiO_2 NPs. From this spectrum, the appearance of a new peak at 636 cm^{-1} indicates the formation of Si-O-Ti surface structures and successful linking of the TiO_2 onto the Fe_3O_4@SiO_2 MNPs. There was no evidence for interaction between Ti and Fe in the IR spectra. It indicates that Fe_3O_4 is encapsulated by the SiO_2 layer well. So, the catalytic property of Fe_3O_4@SiO_2-TiO_2 is not reduced by this interaction.

The magnetization curves of Fe_3O_4, Fe_3O_4@SiO_2 and Fe_3O_4@SiO_2-TiO_2 were recorded in Figure 5. The magnetic property of the Fe_3O_4@SiO_2-TiO_2 magnetic catalyst were examined and were compared with the magnetic properties of $Fe_3O_4$and Fe_3O_4@SiO_2. VSM study indicated a decrease in the magnetic saturation of Fe_3O_4@SiO_2-TiO_2 composite due to the non-magnetic nature of the shell NPs.

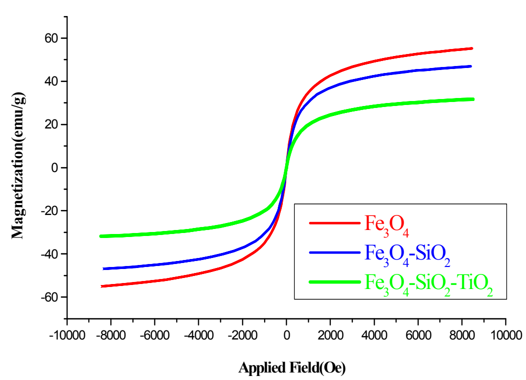

Figure 5. Magnetization curves for the Fe_3O_4 (red line), Fe_3O_4@SiO_2 (blue line) and Fe_3O_4@SiO_2-TiO_2 (green line) at room temperature.

Room temperature specific magnetization versus applied magnetic field curve measurements of the Fe_3O_4@SiO_2-TiO_2 indicated the saturation magnetization value (Ms) of 31 emu g^{-1}, which is slightly lower than of the Fe_3O_4@SiO_2 (46.94 emu g^{-1}) and uncoated Fe_3O_4 MNPs (55.70 emu g^{-1}).

3.2. Application of Fe_3O_4@SiO_2-TiO_2nanocomposite as a heterogeneous catalyst in the synthesis of tetrahydro-[1,2,4] triazolo [1,2-a][1,2,4] triazole-1,5-dithione derivatives.

In this research, we tried to prepare tetrahydro-[1,2,4] triazolo [1,2-a][1,2,4] triazole-1,5-dithione derivatives from the reaction between aldazine derivatives and potassium thiocyanate under mild conditions. Titanium dioxide anchored on the surface of the Fe_3O_4@SiO_2 nanoparticles and carried out successfully the cycloaddition reaction. Initially, in order to optimize the reaction conditions, the model reaction was proceeded from the condensation of benzaldazine and potassium isothiocyanate in a 1:2 ratio at room temperature for the synthesis of compound **3a**using TiO_2, Fe_3O_4 or Fe_3O_4@SiO_2-TiO_2as a catalyst. Fe_3O_4@SiO_2-TiO_2 acted as a highly efficient magnetic catalyst to synthesize perhydro[1,2,4]triazolo[1,2-a][1,2,4] triazole-1,5-dithione (**3a**) and afforded the product in higher yield and lower reaction time compared with other catalysts (Table 1). Also, other advantages of the current catalyst are simple separation and recoverable of Fe_3O_4@SiO_2-TiO_2 compared with reported catalysts. With notice to above results, the importance of Fe_3O_4@SiO_2-TiO_2 composite nanoparticles as a heterogeneous catalyst was revealed in this study and therefore it was selected as the efficient catalyst for further work.

Table 1. The synthesis of tetrahydro-3,7-diphenyl-[1,2,4] triazolo [1,2-a] [1,2,4] triazole-1,5-dithione by various catalysts.

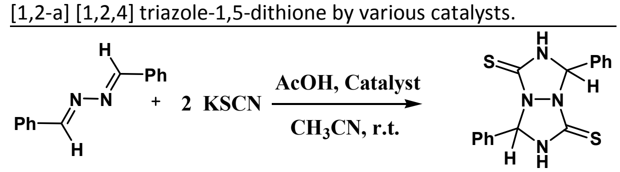

Entry	Catalyst	Yield (%)	Time (min)
1	BF_3	85	21 [Ref. 16]
2	$SbCl_3$	88	21 [Ref. 16]
3	$ZrCl_4$	82	21 [Ref. 16]
4	$TiCl_4$	97	21 [Ref. 16]
5	TiO_2	97	31
6	Fe_3O_4 NPs	96	20
7	Fe_3O_4@SiO_2-TiO_2NPs	98	17

The obtained results of the reaction to determine the optimum amount of magnetic catalyst are shown in Table 2. The reaction slowly proceeded in low yield without catalyst. The higher yield of the corresponding product was obtained in shorter time with an increase in the amount of magnetic nanocatalyst. As can be seen from Table 1, comparison of the results shows a better yield using 0.04 g of catalyst to synthesize of tetrahydro-[1,2,4] triazolo [1,2-a][1,2,4] triazole-1,5-dithiones in the presence of Fe_3O_4@SiO_2-TiO_2. While a higher amount of the catalyst did not show any change in reaction time and yield of the corresponding product.

To demonstrate the advantage of the present work, we compared the results of Fe_3O_4@SiO_2-TiO_2 magnetic catalyst as a catalyst in the synthesis of tetrahydro-[1,2,4] triazolo [1,2-a][1,2,4] triazole-1,5-dithiones in the presence of various solvents (Table 3). It can be

View Article Online
DOI: 10.1039/C5RA23457C

seen from Table 2 that the present CH_3CN was found to be the most efficient solvent among tested solvents in term of reaction time of the desired products in the presence of Fe_3O_4@SiO_2-TiO_2.

Table 2. The synthesis of tetrahydro-3,7-diphenyl-[1,2,4] triazolo [1,2-a] [1,2,4] triazole-1,5-dithione under different amounts of the magnetic catalyst.[a]

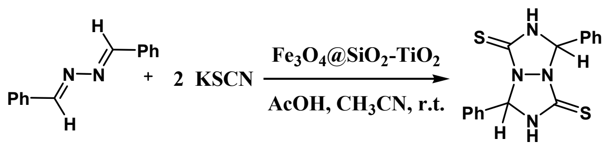

Entry	Catalyst loading (g)	Time (min)	Yield (%)
1	blank	60	32
2	0.01	35	79
3	0.02	23	96
4	0.03	17	97
5	0.04	17	98
6	0.05	17	98

[a] Reaction condition: aldazine (1 mmol), KSCN (2 mmol) AcOH (0.18 mL) and CH_3CN (6 mL) at room temperature.

Table 3. The solvent effects on time and yield of tetrahydro-3,7-diphenyl-[1,2,4] triazolo [1,2-a] [1,2,4] triazole-1,5-dithione in the presence of magnetic catalyst[a].

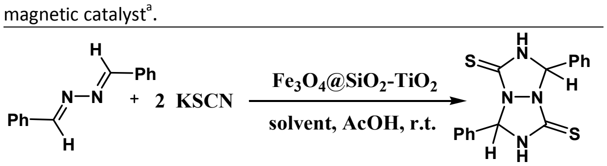

Entry	Solvent	Time (min)	Yield (%)
1	DMSO	20	92
2	CH_3CN	17	98
3	H_2O	25	63
4	EtOH	25	89
5	$CHCl_3$	37	45

[a] The catalyst sonicated for 20 min before utilization.

After establishing the optimal conditions, the scope of the cycloaddition reaction between potassium thiocyanate and several aldazine derivatives were carried out at ambient temperature according to the general experimental procedure (Table 4). As can be seen from this Table, benzaldazine bearing ortho substituent (Table 4, entry 4) slightly afford lower yield than benzaldazines bearing meta or para substituents. This is possibly due to the steric effect. There is more steric hindrance for the 2-substituted benzaldazine on the product formation than the 3- or 4-substituted benzaldazines.

In the case of aldazine derivatives with a hydroxyl group at 2-position (Table 4, entries 9 and 10), the desired products were not synthesized. This is possibly due to tautomeric phenomena of these compounds.

Table 4. The synthesis of tetrahydro-[1,2,4] triazolo [1,2-a][1,2,4] triazole-1,5-dithiones in the presence of Fe_3O_4-SiO_2-TiO_2 MNPs.[a]

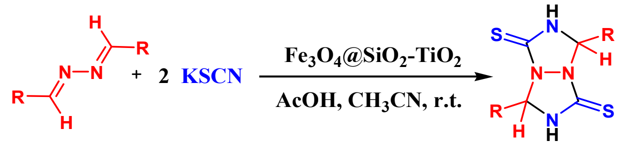

(1) (2) (3)

Entry	R	Product	Time (min)	Yield (%)	M.P. (°C)
1	C_6H_5	3a	17	98	189-190
2	3-NO_2 C_6H_4	3b	30	88	197-199
3	4-OCH_3 C_6H_4	3c	15	98	165-166
4	2-Cl C_6H_4	3d	43	77	190-192
5	3-Cl C_6H_4	3e	20	92	194-196
6	4-Cl C_6H_4	3f	16	94	197-200
7	3-OH C_6H_4	3g	25	90	167-169
8	3-OH, 4-OCH_3 C_6H_3	3h	19	95	170-173
9	2-OH, 4-CH_3 C_6H_3	-	240	-	-
10	2-OH C_6H_4	-	240	-	-

[a] Reaction conditions: aldazine (1 mmol), KSCN (2 mmol), AcOH (0.18 mL), Fe_3O_4-SiO_2-TiO_2 (0.04 g) and CH_3CN (6 mL) at room temperature.

Tetrahydro-[1,2,4] triazolo [1,2-a][1,2,4] triazole-1,5-dithiones as products in a green method were prepared using of potassium thiocyanate and various aldazines in the presence of catalytic amount of Fe_3O_4-SiO_2-TiO_2 MNPs (0.04 g) at room temperature. The structure of the described products was confirmed by physical and spectroscopic data. The infrared spectra of the tetrahydro-[1,2,4] triazolo [1,2-a][1,2,4] triazole-1,5-dithiones exhibits a band at about 3400 cm^{-1} and another band at about 1250 cm^{-1} due to NH and C=S related to the fused five membered rings, respectively. In the ^1H NMR spectra the signal around δ= 8–11 ppm is assigned to NH hydrogen atom.

From a green chemistry perspective, the stability of Fe_3O_4-SiO_2-TiO_2 magnetic catalyst has been investigated by the possibility of reusability. Upon completion of the reaction, to evaluate the catalytic stability of the catalyst, the magnetic catalyst recycled readily by an external magnet, was rinsed with ethyl acetate several times and was dried. It was utilized to a second run of the reaction. The prepared nanocatalyst was stable without the need for surfactant stabilizers. Although the yield decreased from 98 to 96 % after six runs, the catalytic activity was still acceptable (Table 5).

Table 5. The cycloaddition reaction using the recycled Fe_3O_4-SiO_2-TiO_2 magnetic catalyst.

Run	1	2	3	4	5	6	7
Yield (%)	98	98	97	97	97	96	93

View Article Online
DOI: 10.1039/C5RA23457C

3.3. The proposed reaction mechanism

One of the significant advantage of the present catalyst is a large number of empty d-orbitals of the TiO_2 and the low amount of nanocatalyst used in the reaction. The magnetically separable TiO_2 catalyst show great catalytic activity. The features of the Ti^{4+}centres on the surface of TiO_2 nanoparticles play an important role in increasing activation of thiocyanate. In fact, titanium dioxide grafted onto the Fe_3O_4@SiO_2 could catalyze the reaction by the coordination of the unfilled orbitals of TiO_2. Thus, it is obvious that Fe_3O_4@SiO_2-TiO_2 catalytic system increases the rate of reaction.
The formation of the corresponding products can be explained by a proposed mechanism (Scheme 3). According to above reason, enhancing the electrophilic property of the thiocyanate has occurred using titanium dioxide supported on Fe_3O_4@SiO_2. Then, aldazine react as dipoles with two molecules of activated thiocyanate as a dipolarophile to form tetrahydro-[1,2,4] triazolo [1,2-a][1,2,4] triazole-1,5-dithiones.

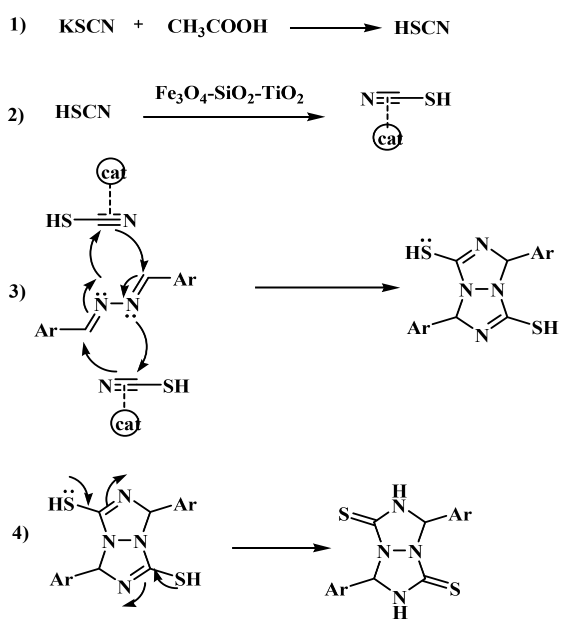

Scheme 3. The proposed mechanism for the synthesis of tetrahydro-[1,2,4] triazolo [1,2-a][1,2,4] triazole-1,5-dithiones using Fe_3O_4@SiO_2-TiO_2.

Conclusions

In this research, we have been described the synthesis of tetrahydro-[1,2,4] triazolo [1,2-a][1,2,4] triazole-1,5-dithiones via condensation of different kinds of aldazine derivatives with potassium isothiocyanate using Fe_3O_4-SiO_2-TiO_2 composite nanoparticles as a magnetic nanocatalyst. The reaction in the presence of recent magnetic catalyst indicated a lot of significant advantages such as eco-friendly and recyclable catalyst, excellent product yields, low reaction times and simplicity of work-up.

Acknowledgements

The authors are grateful to University of Kashan for supporting this work by Grant 256722/XVI.

References

1 Lu Q, Song G, Jasinski JP, A. C. Keeley and W. Zhang, *Green Chem.*, 2012, **14**, 3010–3012.
2 K. V. Gothelf, K. A. Jorgensen and S. Kobayashi, *Wiley-VCH: Weinheim* 2002, 211-247.
3 S. Karlsson and H. E. Hogberg, *Org. Prep. Proceed. Int.* 2001, **33**, 103-172.
4 C. Najera and J. M. Sansano, *Curr. Org. Chem.* 2003, **7**, 1105-1150.
5 J.R. Bailey and N. H.Moore, *J. Am. Chem. Soc.* 1917, **39**, 279-291.
6 H. Zachova´, S. Man, J. Taraba and M. Pota´cˇek, *Tetrahedron* 2009, **65**, 792–797
7 J. Verner and M. Potáček, *Molecules* 2006, **11,** 34–42
8 R. Huisgen, *Angew. Chem., Int. Ed. Engl*. 1963, **2**, 565-598.
9 T. Wagner-Jauregg, *Synthesis* 1976, 349-373.
10 J. G.Schantl, H. Gstach, P. Hebeisen and N. Lanznaster, *Tetrahedron* 1985, **41**, 5525-5528.
11 J.G. Schantl and P. Nadenik, *Synlett.* 1998, **7**, 786-788.
12 H. Kumar, R. Goyal, S. Kaur, R. D. Anand, A. Parmar and B. Kumar, *Indian J. Chem., Sect. B: Org. Chem. Incl. Med. Chem*. 2002, 2182-2184
13 K. Burger, H. Schickaneder, F. Hein, A. Gieren, V. Lamm, H. Engelhardt, *Liebigs Ann. Chem*. 1982, **5**, 845-852.
14 F. J. Hoogesteger, R. W. A. Havenith, J. W. Zwikker, L. W. Jenneskens, K. Huub, N. Veldman and A. L. Spek, *J. Org. Chem*. 1995, **60**, 4375-4384.
15 S. Evans, R. C. Gearhart and E. E. Schweizer, *J. Org. Chem.* 1977, **42**, 452-458.
16 J. Safari, S. Gandomi-Ravandi and M. Ghotbinejad, *J. Korean Chem. Soc.* 2012, **56**, 78-81.
17 J. Safari, S. Gandomi-Ravandi and M. Ghotbinejad,*J. Saudi Chem. Soc.* 2012, http://dx.doi.org/10.1016/j.jscs.2012.02.009
18 T.T. Baby and S. Ramaprabhu, *Talanta* 2010, **80**, 2016–2022
19 A.H. Lv, C. Hu, Y.L. Nie and J.H. Qu, *Applied Catalysis B: Environmental* 2010, **100**, 62–67
20 M. L. Luo, D. Bowden and P. Brimblecombe, *Applied Catalysis B: Environmental* 2009, **87**, 1–8.
21 Y. M. Ren, Q. Dong, J. Feng, J. Ma, Q. Wen and M.L. Zhang, *J. Colloid Interface Sci*. 2012, **382**, 90–96.
22 S. H. Sun, H. Zeng, D. B. Robinson, S. Raoux, P. M. Rice, S. X. Wang and G. X. Li, *J. Am. Chem. Soc.* 2004, **126**, 273–279.
23 Z. D. Zhang, J. G. Zheng, I. Skorvanek, G. H. Wen, J. Kovac, F. W. Wang, J. L. Yu, Z. J. Li, X. L. Dong, S. R. Jin, W. Liu and X. X. Zhang, *J. Physics: Cond. Matt.* 2001, **13**, 1921–1929.
24 S. H. Xuan, F. Wang, X. L. Gong, S. K. Kong, J. C. Yu and K. C. Leung, *Chem. Commun*. 2011, **47**, 2514–2516.
25 A. L. Morel, S. I. Nikitenko, K. Gionnet, A. Wattiaux, J. Lai-Kee-Him, C. Labrugere,B. Chevalier, G. Deleris, C. Petibois, A. Brisson and M. Simonoff, *ACS Nano* 2008, **2**, 847–856.
26 L. Zhou, C. Gao and W.J. Xu, *Langmuir* 2010, **26**, 11217–11225.
27 Z. Q.He, T. M. Hong, J. M. Chen and S. Song, *Separ.Pur. Tech.* 2012, **96**, 50–57.
28 G. H. Du, Z. L. Liu, X. Xia, Q. Chu and S.M. Zhang, *J. Sol-Gel Sci. Tech*. 2006, **39**, 285–291.
29 C. Q. Yang, G. Wang, Z. Y. Lu, J. Sun, J. Q. Zhuang and W. S. Yang, *J. Mat. Chem*. 2005, **15**, 4252–4257.
30 Q. Dai, J. Wang, J. Yu, J. Chen and J. Chen, *Appl. Cat. B: Environmental* 2014, **144**, 686– 693
31 M. Shokouhimehr, Y. Z. Piao, J. Y. Kim, Y. J. Jang and T. Hyeon*Angew. Chem*. 2007, **119**, 7169–73
32 T. Cheng, D. Zhang, H. Li and G. Liu, *Green. Chem.* 2014, **16**, 3401-3427.
33 L. L. Chng, N. Erathodiyil and J. Y. Ying, *Acc. Chem. Res.,*2013, **46**, 1825–1837
34 B. Karimi, F. Mansouri and H. Vali, *Green. Chem.* 2014, **16**, 2587-2596.
35 A. Bamoniri, N. Moshtael-Arani, RSC Adv. 2015, 5, 16911-16920.
36 J. Safari and L. Javadian, *C. R. Chimie*, 2013, **16**, 1165-1171.
37 J. Safari and L. Javadian, *Ultrason. Sonochem*. 2015, **22**, 341-348.
38 H. Naeimi and Z. S. Nazifi, *J. Nanopart. Res*. 2013, **15**, 2026-2036.
39 W. Liyan, W. Hongxia, W. Aijie, and L. Min, *Chin. J. Catatal.* 2009, **30**, 939-944.
40 J. Safari, and S. Gandomi-ravandi, *Synth. Commun*. 2011, **41**, 645-651.

View Article Online
DOI: 10.1039/C5RA23457C

Graphical abstract:

An efficient synthesis of perhydro[1,2,4]triazolo[1,2-a][1,2,4] triazole-1,5-dithiones catalyzed by TiO_2-functionalized nano-Fe_3O_4 encapsulated-silica particles as a reusable magnetic nanocatalyst

Javad Safari and Leila Javadian

Immobilization of a nano-TiO_2 catalyst on the surface of a magnetic SiO_2 support was performed through the reaction of Fe_3O_4@SiO_2 composite with $Ti(OC_4H_9)_4$ *via* a simple process. The Fe_3O_4@SiO_2–TiO_2 nanocomposite was characterized using scanning electron microscopy (SEM), transmission electron microscopy (TEM), energy dispersive X-ray spectroscopy (EDS), X-ray diffraction (XRD), Fourier transform infrared spectra (FTIR), and vibrating sample magnetometer (VSM). The Fe_3O_4@SiO_2–TiO_2 nanocomposite has been found to be an efficient catalyst for the synthesis of perhydro[1,2,4]triazolo[1,2-a][1,2,4] triazole-1,5-dithiones from the condensation of various aldazines and potassium thiocyanate in acetonitrile solvent at room temperature. It has been found that the nanocatalyst was recycled for up to 6 cycles with minimal loss in catalytic activity. The purpose of this research was to provide an easy method for the synthesis of perhydrotriazolotriazole derivatives by a robust and magnetic recoverable catalyst.